The Geometry of Configuration Spaces for Closed Chains in Two and Three Dimensions

R. James Milgram[†]
Department of Mathematics
Stanford University
Stanford California

Jeff Trinkle[‡]
Department of Computer Science
Texas A. and M. University
College Station, TX

In this note we analyze the topology of the moduli spaces of configurations in the plane or three space of all linearly immersed polygonal circles with either fixed lengths for the sides or one side allowed to vary. Specifically, this means that the allowed maps of an n-gon $\langle l_1, l_2, \ldots, l_n\rangle$ where the l_i are the lengths of the successive sides, are specified by an ordered n-tuple of points in $\mathbb{R}^2$, $P_1,\ P_2, \ldots, P_n$ with $d(P_i, P_{i+1}) = l_i$, $1 \leq i \leq n-1$ and $d(P_n, P_1) = l_n$. A similar definition holds in $\mathbb{R}^3$. We show that these configuration spaces are the boundaries of manifolds built out of unions of specific products $(S^1)^H \times I^{n-1-H}$ for the plane, or $(S^2)^H \times I^{2(n-1-H)}$ for three space, over (specific) common submanifolds of the same form. Once the topology is specified, it is indicated how to apply these results to motion planning problems.

§1. Introduction

Polygonal circles in $\mathbb{R}^2$ or $\mathbb{R}^3$ with n-edges are called n-bar mechanisms in mechanical engineering, and they often arise with one of the edges fixed. In the latter case they are called closed $(n-1)$-chains. The space of configurations, particularly in the case of closed chains, is very important in areas like robotics where motions of these mechanisms from an initial position to a final position - often with special constraints like avoiding certain points or some self-intersections - are objects of essential interest. We will describe these connections and related problems in §2.

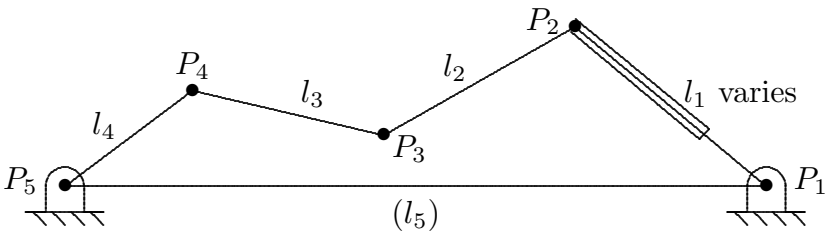

Figure 1: Five bar mechanism with one prismatic joint

The Euclidean group of (oriented) rigid motions, $SE_k = \mathbb{R}^k{:}SO(k)$, for $k = 2,\ 3$ (where $H{:}G$ is the semi-direct product and the action of $SO(k)$ on $\mathbb{R}^k$ is the usual one)

† Partially supported by Sandia National Laboratories and the NSF

‡ Supported by Sandia National Laboratories

acts on these configuration spaces. If we mark an edge and initial point on that edge, the action will bring the image of that edge to a fixed segment, say, for definiteness the segment starting at the origin and lying on the positive x-axis. This action is not necessarily free in $\mathbb{R}^3$ but it is free in $\mathbb{R}^2$. Thus it identifies the configuration space of the n-bar

$$\mathcal{B}(l_1, \ldots, l_n) = \{f : \langle l_1, l_2, \ldots, l_n \rangle \longrightarrow \mathbb{R}^2\}$$

in $\mathbb{R}^2$ with a principal fibration

$$\mathbb{R}^2 : SO(2) \longrightarrow \mathcal{B}(l_1, \ldots, l_n) \longrightarrow \mathcal{C}(l_1, \ldots, l_{n-1} | l_n)$$

where $\mathcal{C}$ is the configuration space of an associated closed $(n-1)$-chain with base edge of length l_n.

To describe the moduli spaces of these maps we identify two such maps if and only if they only differ by the action of an element in these oriented affine groups. For configurations of n-bars or closed chains in $\mathbb{R}^3$, after fixing the image of the base edge we still are allowed to rotate the configuration about the line through P_n and P_1. This gives us an S^1 action on the configuration space of the closed chain (which, generically, is free, but is always semi-free, that is to say the orbits are either free or fixed under the S^1-action) with the fixed point set consisting of a finite set of isolated points - those folded chains where all the segments are co-linear. Thus, generically, the projection of the configuration space of a closed chain in $\mathbb{R}^3$ to the corresponding moduli space is a principal S^1-fibration. (In [KM2] it is shown that in the generic case where the action of $\mathbb{R}^3 : SO(3)$ is free, the quotient manifold has a complex structure. From this it can be shown that the map of the space of configurations where the last edge is mapped to a ray starting at the origin and lying on the positive x-axis to the associated quotient space is a principal S^1-fibration associated to a complex line bundle.)

Remark 1.1: For $\mathbb{R}^2$ we can extend the action to the group of all rigid motions. In this case, generically, the projection of the configuration space of the closed $(n-1)$-chain to the moduli space is a principal $\mathbb{Z}/2$-fibration.

Remark 1.2: For both $\mathbb{R}^2$ and $\mathbb{R}^3$ the configuration spaces depend only on the lengths $l_1, \ldots, l_n$ *and not on their order* up to homeomorphism. Also, in the case where all the lengths are fixed, if we rescale by multiplying all the lengths by the same non-zero constant λ the configuration spaces and moduli spaces are again homeomorphic. Consequently, we can assume that $\sum_1^n l_i = 1$, all the $l_i > 0$, and if we wish, that the lengths are given in increasing order. *Unless otherwise stated this convention will be in force for the remainder of this note whenever we discuss the situation where all the lengths are fixed.*

Definition 1.3: *Assume that the l_i are normalized as above. Then we say that the subset $V = (l_{i_1}, l_{i_2}, \ldots, l_{i_r})$ consists of* **long links** *if and only if the sum of any two lengths in V is greater than $\frac{1}{2}$. The cardinality of V can be at most three.*

The following lemma appears in [KM1] and shows that no real n-bar can have only one long link:

LEMMA 1.4: *The ordered sequence* $\langle l_1, l_2, \ldots, l_n\rangle$ *with* $\sum_1^n l_i = 1$ *and* $l_i > 0$ *for all* i*, has a non-empty configuration space in* $\mathbb{R}^2$ *if and only if each* $l_i \leq \frac{1}{2}$.

(The proof is elementary. The result is verified for $n = 3$ and then the proof for $n > 3$ is a direct induction when one observes that for $n > 3$, there must be two lengths l_i, l_j with $l_i + l_j < \frac{1}{2}$.)

Sometimes these moduli spaces of configurations will have non-manifold points, but generically, they are manifolds. The conditions for singularity are precisely described in [KM1] and will be reviewed in §4, §5. Here is our first main result.

THEOREM 1.5: *Let* $\mathcal{M}$ *be a closed* $(n-1)$*-chain with lengths*

$$l_1, l_2, \ldots, l_{n-1}$$

and base length l_n.

(a) Except for a finite number of l_n, $\mathcal{C}(\mathcal{M})$ *is a closed compact manifold of dimension* $(n-3)$ *for* $\mathbb{R}^2$ *and* $(2n-5)$ *for* $\mathbb{R}^3$.

(b) Whenever $\mathcal{C}(\mathcal{M})$ *is a manifold, it is the boundary of a manifold* W^{n-2} *for* $\mathbb{R}^2$ *or* W^{2n-4} *for* $\mathbb{R}^3$ *which is given as a union of sub-manifolds of the form*

$$(S^1)^s \times I^{n-s-2} \text{ for } \mathbb{R}^2,\ (S^2)^s \times (I^2)^{n-s-2} \text{ for } \mathbb{R}^3.$$

(The set of s *that occur depend on the lengths in a fairly direct way.)*

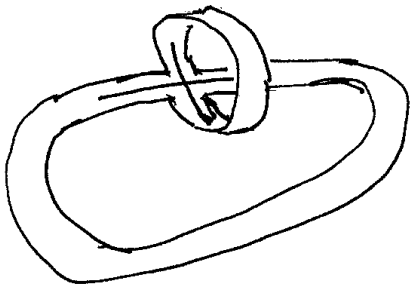

Figure 2: The (coordinate) union of two copies of $S^1 \times I$

This union is constructed as follows. Whenever two such pieces intersect, their intersection is a common (coordinate) sub-manifold of the form $(S^1)^l \times I^{n-l-2}$ *for* $\mathbb{R}^2$ *or* $(S^2)^l \times I^{2(n-l-2)}$ *for* $\mathbb{R}^3$.

Here, coordinate sub-torus simply means that we fix a finite number of the product coordinates in $(S^1)^{n-1}$ for $\mathbb{R}^2$ or $(S^2)^{n-1}$ for $\mathbb{R}^3$ and allow the remaining points to vary over all possible values. Also, the structure of this finite union of sub-tori (or products of S^2's)

is entirely explicit, consisting of a finite number of maximal sub-tori together with *all their possible intersections*, and the set of maximal sub-tori is given in the body of the paper as a combinatorial function of the lengths.

REMARK 1.6: In specific cases, it is quite direct to determine the exact structure of these W^{n-2} or $W^{2(n-2)}$.

EXAMPLES 1.7: We give some examples for $\mathbb{R}^2$. The situation is similar in $\mathbb{R}^3$.

(a) If all the l_i, $i < n$, are equal, then the only possible W^{n-2} are thickenings of the full s-skeleton of $(S^1)^{(n-1)}$ for $s \leq [(n-1)/2]$.

(b) If there are three long edges, the thickening is

$$(S^1)^{n-3} \times I.$$

(c) If there are two long edges, the space $\mathcal{C}(\mathcal{M})$ is the double over the boundary of one of these thickenings, more exactly:

THEOREM 1.8: *Suppose all the edges have fixed length, suppose that the assumptions of the above theorem are satisfied, and suppose, moreover, that there are two "long edges", l_i and l_j, $(i \neq j)$, so that $l_i + l_j > \frac{1}{2}$. Then the configuration space for the associated n-bar mechanism is the double along the boundary of a thickening having the type described in the previous theorem for $\mathbb{R}^2$.*

(d) REMARK 1.9: The description of the associated configuration spaces in $\mathbb{R}^3$ is somewhat more complicated, though it is still a double.

(e) In the general case, the moduli space of configurations of a fixed-length n-bar mechanism in the plane is the double of a thickening of the type above *minus the thickening of a neighborhood of a union of coordinate sub-tori* contained in it. *But these differences of thickenings are, themselves, the moduli spaces of embeddings when one edge is allowed to vary in length between two fixed values, $0 \leq a < l_1 < b$.*

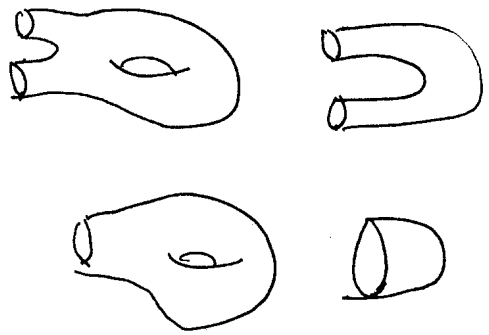

Figure 3: Thickenings with boundaries $\mathcal{C}$-spaces for 4-bars

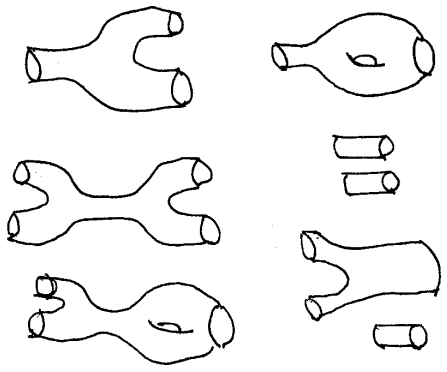

Figure 4: The differences of the thickenings above

Moreover, from the description above, the intersection pairing is easily described in any specific case, so the homology structure of the $\mathcal{C}(\mathcal{M})$ can be regarded as completely known for any closed chains in $\mathbb{R}^2$ with no obstacles.

These thickenings are also the building blocks for constructing the configuration spaces themselves in the case of $\mathbb{R}^2$. In fact, the configuration spaces for fixed-length mechanisms are simply doubles along the boundary of a certain associated W^{n-2} or the difference of two such, W^{n-2} and $W'^{(n-2)} \subset W^{n-2}$. On the other hand, these differences are *precisely* the configuration spaces of mechanisms where the length of exactly one edge is allowed to vary between two finite values

$$0 \leq l(0) \leq l_n \leq l(1) \leq \sum_1^{n-1} l_j,$$

and this is true for both $\mathbb{R}^2$ and $\mathbb{R}^3$.

REMARK 1.10: It is also possible for the mechanism to have three long edges l_i, l_j, l_k so that the sum of any two is $\geq \frac{1}{2}$, though it is not possible to have four long edges. In the case of three long edges we have the important result, [KM1]:

THEOREM 1.11: *For configurations of an n-bar mechanism with fixed lengths in $\mathbb{R}^2$ the configuration space is connected if and only if the mechanism does not have three long edges. Moreover, in the case where the mechanism does have three long edges, then the configuration space has exactly two components and each component is a torus $(S^1)^{n-3}$. (In $\mathbb{R}^3$ the moduli space is always connected.)*

The explicit descriptions of the configuration spaces given above allow for very efficient motion planning in these thickened regions or differences of thickened regions. Specifically, when the topology of the region is sufficiently well understood, it is possible to construct efficient (piecewise geodesic with very few breaks) paths in polynomial time, (roughly vn^4) where v is a constant that depends on the specific configuration space.

Also, the determination of the relevant aspects of the topology of these regions can be done in roughly 2^{3n} steps (which is best possible in general, though when there are very

few distinct lengths, the number is much smaller). Of course, this latter calculation need only be done once.

The authors have used these results to develop a *complete* program for motion planning for closed chains that works in polynomial time independent of whether the topology is well understood. The trade off is that these paths may be quite far from optimal. (Here complete means that if it is possible to find a path from the initial configuration to the final configuration, the program will construct one, and if it is not possible, the program will report this as well.)

These closed n-chains are a special family of linkages. Over the years, quite a number of papers have been written that deal with aspects of the problem of determining the configuration spaces and moduli spaces of linkages. It is known, as was shown by Thurston (unpublished, but see [KM3]), that the complexity of the full subject is that of real algebraic geometry, though, as the results above show, the situation becomes much more manageable when we restrict to special families. Most recently the results of [KM1], [KM2], [KM3], provide a good review of previous work and give a number of interesting results on the structure of these configuration spaces, particularly the configuration spaces for closed chains in $\mathbb{R}^2$ and $\mathbb{R}^3$.

In further work, the authors expect to discuss extensions of the results above to configuration spaces for closed chains in the presence of obstacles and constraints. Also, we would like to thank Steven Kaufman for all the help and encouragement he gave us throughout the development of these results.

§2: Background

Kinematics is the study of the possible motions of systems of bodies coupled mechanically through contact constraints. These constraints can be permanent, as in the case of a hinge joint, or intermittent, as in the case of a ratchet mechanism. A common problem in mechanism design is to choose the number of links and their lengths, twists, and offsets, so as to allow a particular link to move (relative to a given base link) from one configuration to another, possibly following some specified rigid body motion. Currently, this design problem is solved taking little or no advantage of the structure of the space of configurations of the mechanisms under consideration. While some research results that leverage global structure of the configuration spaces have appeared in the literature †, common design practices still tend to rely on iterative numerical procedures that use only local information. As a result, the design process for mechanisms with even small numbers of joints is tedious.

In the design of common one-degree-of-freedom mechanisms, such as the four-bar linkage and crank and slider mechanisms, [H], current design tools are reasonably powerful and efficient. However, the field of robotics has been placing increasingly difficult demands on mechanism designers. Most robotic applications require more degrees of freedom from mechanisms than current design tools can readily handle. One challenging class of robotics

† For example, Shukla and Mallik, [SM], developed a method to determine the existence of a crank (a link that can rotate 360^o relative to some other link in Watt and Stephenson chains (six-bar, planar mechanisms with two loops)).

problems requires the motion planning and control of a closed-chain mechanism with many degrees of freedom. For example, a bomb-disposal robot must be capable of moving to a door (behind which is a bomb), and opening it. While the robot is opening the door, a closed kinematic chain is formed that is composed of the robot arm and the door, connected to the ground at either end. To open the door, one must understand the constraints imposed on the system by the kinematic loop and be able to plan the motion of the system from an initial state (the door is closed) to a goal state (the door is fully open).

Despite the fact that bomb-disposal and many other robotic tasks require good designs and motion planning for closed kinematic chains, the state of the art is surprisingly crude. The most effective robot motion planners today are built upon randomized search techniques. [KLOS], [WXH]. However, individual randomized techniques have wildly varying performance and are not complete; they are not guaranteed to find a solution when one exists, nor can they determine that a solution does not exist when that is the case. The theoretical basis for a complete general motion planner was developed roughly 15 years ago, [C], but it has never been implemented due to the complexity of the specified algorithms.

The work presented here represents a first step in the development of maximally efficient, complete motion planners for robotic mechanisms. More importantly, the work expands the field of theoretical kinematics. Previously, the only mechanisms for which the global properties of configuration space were understood, were those of planar mechanisms with very small numbers of joints (e.g., the four-bar mechanism). Here we completely determine the global structure of configuration spaces of spatial n-bar mechanisms, where n is arbitrary. The class of mechanisms considered are those forming a single closed loop. For planar mechanisms, all joints are of the type know as "revolute" (i.e., hinge joints); they constrain adjacent links in the loop allowing only relative rotation about the axis of the joint. For spatial mechanisms, all links are connected by "U"-joints (i.e., pairs of revolute joints with intersecting axes). In addition, one link is allowed to change its length (i.e., the mechanism may have one prismatic joint). While our analysis allows self-intersection of the links, once the associated configuration space is understood, there are standard methods in topology for dealing with restrictions on the embeddings so that, for example, there are no self-intersections or the mechanisms do not intersect given closed sets in $\mathbb{R}^2$ or $\mathbb{R}^3$. We will not discuss these techniques here, but expect to do so in subsequent work.

§3: Planning Paths in the Configuration Space

Briefly, assume that we are given two points, A and B, in the configuration space of a closed chain in $\mathbb{R}^k$, $k = 2$ or 3, with the last edge based at $\vec{0}$ and lying on the x-axis. Then the space of paths from A to B is homotopy equivalent to the loop-space $\Omega(\mathcal{B}(l_1, \ldots, l_n))$ (if A and B lie in the same path-component) or it is empty. Consequently, for $n \geq 4$, if the path space is not empty, then there are many ways of moving from A to B. Given the non-uniqueness of paths and the huge difficulty, in general, of determining geodesics between A and B, one must identify the most important path attributes to guide their construction.

If any path between A and B will do, then one may proceed a step at a time. Using 1.11, we can check whether we are dealing with a path connected space or one that has two components. If there are two components, then they are distinguished by the relative positions of the three long links. For example, if the long links are l_2, l_3 and l_4 (as in Figure 5), then $\{l_3\}$ will be in one half-plane or the other relative to l_4.

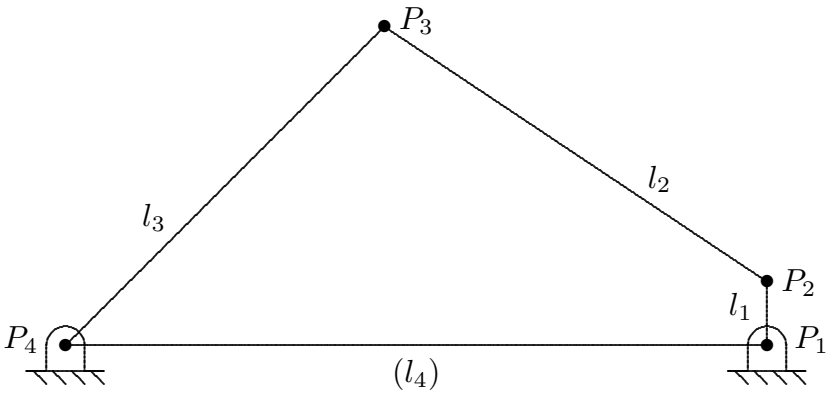

Figure 5: A four-bar mechanism with three long links.

Since in the case of two components, the short links are free to move in any way, the configuration space is comprised of two tori. Hence the motion planning algorithm here is very simple, determine if A and B are in the same component and, if so, move the short links in a straight line on the torus from their configuration for A to their configuration for B.

In the case of a single path connected component, one can simply move one link after another into the correct position, and then fix it. Having fixed a link, we can lump it with the old base link to form a new base link leaving a closed chain with one less link. The next move will be from the configuration just achieved, A_k, to the original goal configuration, B. Before beginning the next move, however, one checks the number of components in configuration space of the reduced chain. If there are two components and A_k and B are in the same component, proceed as in the previous paragraph. If they are not in the same component, we adjust the previous move to ensure that the long links move into the correct relative position before moving the next link into its correct final position.

Such algorithms take advantage only of our knowledge of the path components and our ability to detect which component contains a given configuration. But we also know much more about the geometry and topology of the configuration space than just the components. It turns out that the tori $T^s \times pt \subset T^s \times I^{n-s-2}$ in our W's are very close to geodesic, so when design constraints permit, it is quite efficient to locate one of these tori close to A, another close to B. This done, one can plan the path by constructing a path in the poset of the T^s from the first torus to the other. Of course, this requires that one do a potentially very long analysis of a certain set of critical radii given explicitly in the statement of 5.1. Algorithms for doing this can be extracted from the discussion that follows 7.8.

§4: Constructing Configuration Spaces of Closed Chains

In this section we restrict ourselves to $\mathbb{R}^2$. It is direct to extend the discussion to $\mathbb{R}^3$ however. Also, before we do the analysis of the closed situation, we consider open chains (where one end-point is allowed to vary but the other is fixed).

For open chains the structure of the configuration space is clear: a chain's configuration is determined by the successive angles between the edges, and between the base edge and some fixed ray emanating from the base-point. Consequently, the configuration space of an open chain with m segments is just the m-torus $(S^1)^m$.

We also need to consider the workspace of an open chain. This consists of all the points in the plane that occur as the image of the free end-point of the chain. For example, in the case of an open chain with two unequal edges the workspace is always an annulus centered at the fixed end-point, with outer circle of radius $l_1 + l_2$ and inner circle of radius $|l_1 - l_2|$.

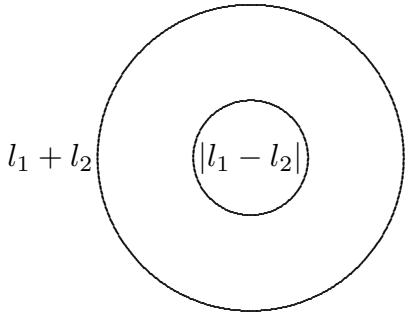

Figure 6: Annular Workspace for Two-Edge Linkage

Here, it is also worth noting that there are exactly two configurations with a given end-point as long as the end-point is in the interior of the annulus, while the configurations on the boundary circles occur only when the two edges lie on a *single* line through the base-point. In the case where the two edges have equal length the workspace is the entire disk of radius $2l_1$, but the inverse image of the base-point in the configuration space consists of an entire circle.

In the case of an open chain with a single edge of length l, the workspace is just the circle of radius l centered at the base-point, while the workspace for a general open chain with at least three links is either the closed annulus or the closed disk centered at the origin. In both cases the outer radius will be $\sum_i l_i$.

Let us consider the configuration space of *closed chains* with three segments, i.e., planar 4-bar mechanisms. To do this we consider simultaneously an open chain with one edge of length l_3 based at P_4 and an open chain with two edges of lengths l_1 and l_2, based at P_1. Assume, for the moment that P_1 and P_4 are further apart than $l_1 + l_2 + l_3$, so there is no configuration of the closed chain that connects P_1 and P_4. Then start moving P_4 towards P_1 till the edges of the workspaces touch as shown in Figure 7:

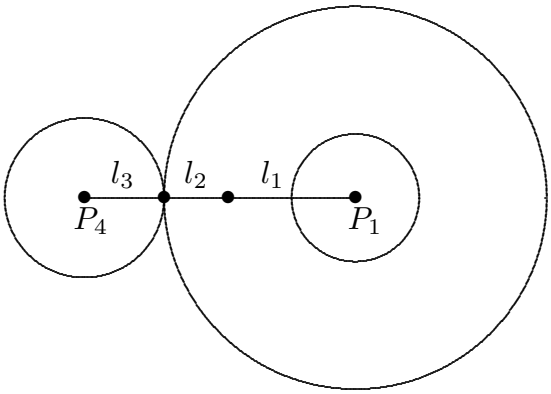

Figure 7: Workspaces Just Touching

Now there is a single solution – the three edges lie along the line containing P_1 and P_4. Continue to move P_4 towards P_1, so the intersection of the workspaces is an arc whose interior is completely contained in the interior of the annular workspace of the 2-chain. At each interior point $\vec{v}$ of the arc there are exactly two configurations of the 2-chain at P_1 with $\vec{v}$ locating the free end-point. At each end-point of the arc there is only one configuration of the 2-chain. Consequently, for the region defined by

$$l_1 + l_2 > ||P_1 - P_4|| - l_3 > |l_1 - l_2|$$

(provided that $||P_1 - P_4|| > l_1 + l_2 - l_3$) the configuration space is simply a circle. (Four-bar mechanisms satisfying the condition that their configuration space is a single circle are referred to as *non-Grashof* in the engineering literature.)

The configuration space continues to be a circle as P_4 moves towards P_1 until either the arc of intersection touches the interior circle of the annulus (or P_1 when the interior circle is degenerate, *i.e.*, $l_2 = l_1$), (which will occur if $2l_3 > |l_1 - l_2|$)

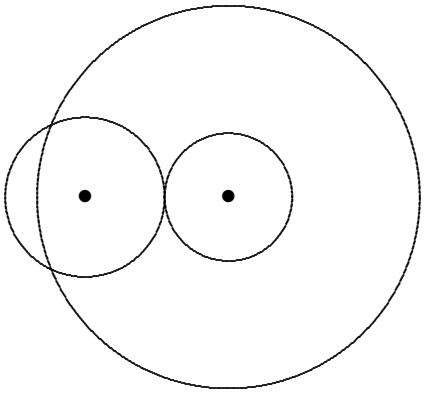

Figure 8: Workspaces Just Touching at Inner Boundary

or the intersection becomes the entire circle, with one point tangent to the outer circle of the annulus (which can only happen if $2l_3 < |l_1 - l_2|$). Mechanisms with this type of configuration space are known in the engineering literature as *uncertain* since the inverse

image of motion through the singular point given by three colinear links bifurcates.

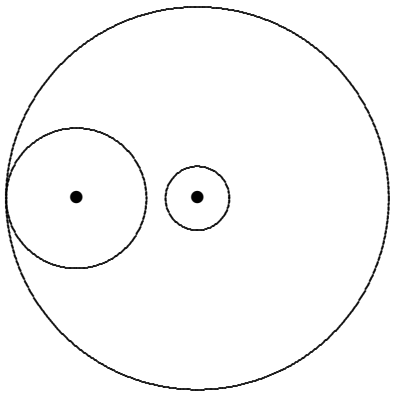

Figure 9: Workspace Contained and Touching Outer Boundary

In both these cases the configuration space becomes a figure 8, while in the degenerate case (occurring when $2l_3 = |l_1 - l_2| > 0$), we find that the configuration space becomes the following graph:

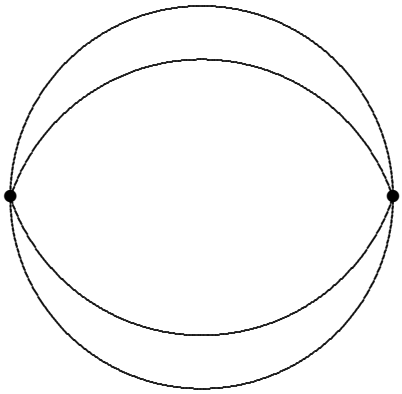

Figure 10: Three Loop Graph With Two Vertices

The remaining case occurs when the arc becomes tangent to the inner and outer circles of the annulus simultaneously *and*, the inner circle degenerates to the point P_1, *i.e.*, $l_1 = l_2 = l_3$. In this case the configuration space is a three vertex, six edge graph, with four edges incident on each vertex.

As P_4 continues to move towards P_1 various possibilities now occur. The two most important are represented in continuing the situations in both Figure 8and Figure 9, where, in two different ways - as the circle crosses the inner radius in Figure 8, or becomes entirely contained in the interior of the annulus for Figure 9- the configuration space becomes two disjoint circles. In the engineering literature, this is referred to as *Grashof*, and represents the usual way in which four-bar mechanisms are applied.

The reader can easily list the remaining possibilities. A similar analysis can be done for five bar mechanisms, and such an approach is discussed in [KM1]. There are exactly six non-singular closed surfaces that appear as configuration spaces for 5-bar mechanisms, the

surfaces of genus ≤ 4 and the disjoint union of two copies of the torus $S^1 \times S^1$. However, as the number of bars increases, this approach becomes too complex, and we need more systematic and powerful methods.

§5: Generic points for the map to the workspace

The considerations above indicate that it should be possible to "bootstrap" from n-bars to $(n+1)$-bars, provided we understand the entire configuration space for the lengths $l_1, l_2, \ldots, l_{n-1}$ in the sense that we know the inverse image of any point in the workspace. In doing this, we introduce the intersection of the circle of radius l_n and the workspace, provided that the center of this circle is at distance l_{n+1} from the origin. Then the configuration space of the $(n+1)$-bar is the inverse image of this intersection.

Also, the considerations above indicate that there are certain critical circles in the workspace, those circles where the inverse image contains a configuration with all the edges colinear, and that the inverse image will be non-singular unless the circle of radius l_n is *tangent* to one of these critical circles.

Both of these results are true. In fact, even more is true. If we choose an initial point on the circle and take the (signed) distance on the component of the intersection of the circle of radius l_n with the workspace that contains the initial point, as a function on the inverse image of the configuration space, then this function is *locally* Morse, with all its critical points contained in the inverse images of the intersection of this circle with the critical circles in the workspace.

Here are the basic results.

THEOREM 5.1: *Let $\vec{q}$ be any point in the workspace of the open chain with lengths*

$$\langle l_1, l_2, \ldots, l_n \rangle,$$

then the inverse image of a point p in the torus $(S^1)^n$ is an $(n-k)$ dimensional manifold (where $k = 2$ if we are in $\mathbb{R}^2$ and $k = 3$ if we are in $\mathbb{R}^3$) if and only if p is not on one of the circles (spheres), centered at the center of the workspace having radius $R_I = |\sum l_i - 2\sum_{j\in I} l_j|$ where $I \subset \{1, 2, \ldots, n\}$ is any subset.

THEOREM 5.2: *Suppose that $\vec{0}$ is not a critical circle (sphere). Suppose that $P(x, y) = 0$ or $\{g(x, y, z) = h(x, y, z) = 0\}$, depending on whether we are in $\mathbb{R}^2$ or $\mathbb{R}^3$, defines a C^∞ rectifiable curve γ in the workspace. Then the inverse image of γ is non-singular if and only if γ is transverse to each of the critical circles (spheres) that it intersects.*

(Here the critical circles and spheres are the spheres described in the result above.)

COROLLARY 5.3: *Let R_I and R_J be adjacent critical radii, and $W(I, J)$ the open annulus (in $\mathbb{R}^2$) or open spherical shell (in $\mathbb{R}^3$) between them, then the map of the inverse image of $W(I, J)$ onto $W(I, J)$ is a trivial fibration.*

As a consequence, if the curve γ lies entirely in one of the $W(I, J)$, then the inverse image of γ is also a product $I \times V$ where V is the inverse image of an arbitrary point in $W(I, J)$, and it follows that any two γ which lie entirely in $W(I, J)$ have diffeomorphic inverse images.

THEOREM 5.4: *Suppose that the curve γ in the workspace satisfies the properties above for non-singularity of the inverse image, and, again, $\vec{0}$ is not a critical circle (sphere). Then*

arc length on γ is locally a Morse function with critical points exactly the points in the inverse images of γ intersected with the critical circles (spheres) where all the edges are co-linear.

In the next two sections we give the proofs.

§6: The proofs of the general position theorems above

We now give a proof of these facts in three dimensions, though the arguments are virtually identical (but more direct) in two dimensions.

LEMMA 6.1: *The map f which sends an open chain with lengths $l_1, \dots, l_{(n-1}$, based at 0 to its endpoint has as its critical points precisely the spheres centered at the origin of radius $|\sum_{i=1}^{n-1}(-1)^{e_i} l_i|$ where the $(n-1)$-tuples $(e_1, \dots, e_{(n-1)})$ run over all $2^{(n-1)}$ possiblities with each $e_i \in \{0, 1\}$.*

EXAMPLE 6.2: If $(l_1, l_2, l_3, l_4) = (1, 1.5, 2, 3)$ then there are exactly six critical radii, .5, 1.5, 2.5, 3.5, 4.5 and 7.5 with 1.5 and 2.5 occuring in four distinct ways, and each of the others in 2 distinct ways.

PROOF: We consider chains in three dimensions given in the form of the following set of equations:

$$\begin{aligned} x_i^2 + y_i^2 + z_i^2 &= 1,\ 1 \le i \le n-1 \\ \sum_1^{n-1} l_i x_i &= 0 \\ \sum_1^{n-1} l_i y_i &= 0 \\ \sum_1^{n-1} l_i z_i &= l_n \end{aligned}$$

The first set of constraints defines the product $(S^2)^{n-1}$, which is non-singular and has tangent space just the product of $n-1$ copies of the tangent space to S^2. Precisely, the space of tangent vectors at the point $(\vec{X}_1, \dots, \vec{X}_{n-1})$ is the set of all vectors $(\vec{P}_1, \dots, \vec{P}_{n-1})$ with $\vec{P}_i \perp \vec{X}_i$, $1 \le i \le n-1$, $\vec{P}_i \in \mathbb{R}^3$. The map *(forward kinematics map)*

$$f\colon (\vec{X}_1, \dots, \vec{X}_{n-1}) \longrightarrow \mathbb{R}^3 \tag{6.3}$$

defined as $f(\vec{X}_1, \dots, \vec{X}_{n-1}) = \sum l_i \vec{X}_i$ induces the tangent map

$$df\colon (\vec{P}_1, \dots, \vec{P}_{n-1}) = \sum l_i \vec{P}_i \tag{6.4}$$

and this map is onto except when the tangent spaces to the different $\vec{X}_i$ are all the same, which happens if and only if $\vec{X}_i = \pm \vec{X}_1$, $1 \le i \le n-1$.

Thus, if the point $\begin{pmatrix} 0 \\ 0 \\ l_n \end{pmatrix}$ does not lie on one of the critical spheres, it is a regular point, and conversely. ∎

COROLLARY 6.5: *Let V be the open annular region between two of successive critical spheres in the situation above. Then the inverse image of V is the product $V \times f^{-1}(v_0)$ for any $v_0 \in V$.*

PROOF: The action of the orthogonal group O_3 based at the origin, preserves the map f, but since there are no critical points in V and the inverse image of every point is compact, it follows that the map is a fibration. ∎

Let γ be any rectifiable curve embedded in the workspace, and suppose that W is the inverse image of γ under f.

COROLLARY 6.6: *Suppose that either $\vec{0}$ is not a critical radius or that γ does not contain $\vec{0}$. Then W is a differentiable manifold if and only if γ intersects each critical sphere transversally. Moreover, if W is differentiable, and γ satisfies these assumptions, then the set of critical points of the composition of the length function on γ with f on W is exactly the set of $(\vec{X}_1, \ldots, \vec{X}_{n-1}) \in W$ where all the $\vec{X}_i$ are colinear.*

PROOF: We assume that the end of the chain is constrained to run along a curve given in a small neighborhood of point of interest, which we assume is on a critical sphere, by the pair of equations

$$\begin{aligned} p(x,y,z) &= 0 \\ q(x,y,z) &= 0. \end{aligned}$$

Setting $x = \sum l_i x_i$, $y = \sum l_i y_i$, $z = \sum l_i z_i$, putting

$$A_x = \frac{\partial p}{\partial x}\ A_y = \frac{\partial p}{\partial y}\ A_z = \frac{\partial p}{\partial z}$$

and similarly

$$B_x = \frac{\partial q}{\partial x}\ B_y = \frac{\partial q}{\partial y}\ B_z = \frac{\partial q}{\partial z}$$

we have that the tangent line to the curve at $\vec{X}$ is the kernel of the Jacobian matrix

6.7
$$J_\gamma = \begin{pmatrix} A_x & A_y & A_z \\ B_x & B_y & B_z \end{pmatrix}.$$

Also, the derivative of the length function is the dot product of the unit tangent vector in the direction of increasing s with the image of df from $\tau(W)$ to $\tau(\gamma)$.

We have that the Jacobian for the resulting variety W near $f^{-1}(\vec{X})$ is given as

6.8
$$J_C = \begin{pmatrix} 2x_1 & \ldots & 0 & 2y_1 & \ldots & 0 & 2z_1 & \ldots & 0 \\ \vdots & \ddots & \vdots & \vdots & \ddots & \vdots & \vdots & \ddots & \vdots \\ 0 & \ldots & 2x_{n-1} & 0 & \ldots & 2y_m & 0 & \ldots & 2z_{n-1} \\ A_x l_1 & \ldots & A_x l_{n-1} & A_y l_1 & \ldots & A_y l_{n-1} & A_z l_1 & \ldots & A_z l_{n-1} \\ B_x l_1 & \ldots & B_x l_{n-1} & B_y l_1 & \ldots & B_y l_{n-1} & B_z l_1 & \ldots & B_z l_{n-1} \end{pmatrix}$$

Looking at the restriction of this matrix to the tangent vectors to $(S^2)^{n-1}$ we get image vectors of the form

$$\begin{pmatrix} 0 \\ \vdots \\ 0 \\ J_\gamma \sum l_i \vec{T}_i \end{pmatrix}$$

with $(\vec{T}_1, \ldots, \vec{T}_{n-1})$ in the tangent space at $(\vec{X}_1, \ldots, \vec{X}_{n-1})$. The only way the rank of this image can be less than full is if all the $\vec{T}_i$ lie in the same plane, and the tangent to γ lies in this plane as well.

On the other hand, at a point where all the $\vec{X}_i$ are colinear, the tangent plane is the kernel of J_C, and this is the set of vectors which are, first $\perp \vec{X}_1$, and second, annihilated by J_γ. But since J_γ restricted to $\perp \vec{X}_1$ is an isomorphism, this shows that the tangent space at this critical point is exactly the space of $(n-1)$-tuples

$$\left[(\vec{T}_1, \ldots, \vec{T}_{n-1}) \;\middle|\; \vec{T}_i \perp \vec{X}_1, \sum_1^{n-1} l_i \vec{T}_i = \vec{0} \right].$$

Thus we have identified the critical points of f restricted to $f^{-1}(\gamma)$ as the set of elements in $f^{-1}(\gamma)$ where all the $\vec{X}_i$ are colinear. ∎

Thus we have shown that under the assumptions above, the length function $s_\gamma f$ restricted to W has isolated critical points. It remains to analyze the Hessian at these critical points to prove that this function is Morse.

We do this in the case of $\mathbb{R}^2$, the case of $\mathbb{R}^3$ being similar.

We assume that $w_1, \ldots, w_{n-2}$ are the local coordinates where w_i is the angle that the i^{th} segment makes with the x-axis, and $w_{n-1} = w_n(w_1, \ldots, w_{n-2})$. Then, if $\vec{X}_i = \begin{pmatrix} x_i \\ y_i \end{pmatrix}$ and $\vec{X} = \sum_1^n l_i \vec{X}_i$ we have

$$\frac{\partial^2}{\partial w_i^2} X = -l_i \vec{X}_i - l_{n-1} \frac{\partial w_{n-1}}{\partial w_i^2} \vec{X}_{n-1}$$

while

$$\frac{\partial^2}{\partial w_i \partial w_j} \vec{X} = -l_{n-1} \frac{\partial w_{n-1}}{\partial w_i \partial w_j} \vec{X}_{n-1}$$

for $i \neq j$. Consequently, since we are at a critical point and the $\vec{X}_i$, $i = 1, \ldots, n$ are all co-linear, the determination of the Hessian matrix reduces to the determination of the second derivatives $\frac{\partial^2 w_n}{\partial w_i \partial w_j}$ and the specification of a sign for each $\vec{X}_i$. We omit the details of this calculation as they are direct and record only the result: The Hessian matrix, H, at the critical point becomes

$$\begin{pmatrix} (-1)^{j(2)} l_2 l_j + l_2^2 & (-1)^{j(2)+j(3)} l_2 l_3 & \ldots & (-1)^{j(2)+j(n-2)} l_2 l_{n-2} \\ (-1)^{j(2)+j(3)} l_2 l_3 & (-1)^{j(3)} l_3 l_j + l_3^2 & \ldots & (-1)^{j(3)+j(n-2)} l_3 l_{n-2} \\ \vdots & \vdots & \ddots & \vdots \\ (-1)^{j(2)+j(n-2)} l_2 l_{n-2} & (-1)^{j(3)+j(n-2)} l_3 l_{n-2} & \ldots & (-1)^{j(n-2)} l_{n-2} l_j + l_{n-2}^2 \end{pmatrix}$$

LEMMA 6.9: *The Hessian above is non-singular if and only if the sum*

$$K_{n-1} \;=\; \sum_1^{n-1} (-1)^{j(i)} l_i$$

is non-zero. In this case, if the intermediate sums $K_k = \sum_1^k (-1)^{j(i)} l_i$ *are all non-zero, then the index of the Hessian is* $\pm$ *the number of sign changes in the sequence,* $(-1)^{j(1)+j(2)+\cdots+j(k)} K_k$ *for* $1 \leq k \leq m$. *(Explicitly, the first few terms of the sequence are* l_1, $(-1)^{j(1)+j(2)}((-1)^{j(1)} l_1 + (-1)^{j(2)} l_2)$, $(-1)^{j(1)+j(2)+j(3)}((-1)^{j(1)} l_1 + (-1)^{j(2)} l_2 + (-1)^{j(3)} l_3)$.*)*

PROOF: In a neighborhood of the critical point write $\theta_i = \frac{\pi}{2}(1 - (-1)^{j(i)}) + (-1)^{j(i)}\delta_i$, so the δ_i become local coordinates. We assume that δ_1 can be given in terms of the remaining coordinates, and set

$$V^t = (\delta_2, \delta_3, \ldots, \delta_{n-1}),$$

$$C = \begin{pmatrix} (-1)^{j(2)} l_1 l_2 & 0 & 0 & \ldots & 0 \\ 0 & (-1)^{j(3)} l_1 l_3 & 0 & \ldots & 0 \\ 0 & 0 & (-1)^{j(4)} l_1 l_4 & \ldots & 0 \\ \vdots & \vdots & \vdots & \ddots & \vdots \\ 0 & 0 & 0 & \ldots & (-1)^{j(m)} l_1 l_{n-1} \end{pmatrix}$$

and

$$RR^t = \begin{pmatrix} l_2^2 & (-1)^{j(2)+j(3)} l_2 l_3 & \ldots & (-1)^{j(2)+j(n-1)} l_2 l_{n-1} \\ (-1)^{j(2)+j(3)} l_2 l_3 & l_3^2 & \ldots & (-1)^{j(3)+j(n-1)} l_3 l_{n-1} \\ \vdots & \vdots & \ddots & \vdots \\ (-1)^{j(2)+j(n-1)} l_2 l_{n-1} & (-1)^{j(3)+j(n-1)} l_3 l_{n-1} & \ldots & l_{n-1}^2 \end{pmatrix}$$

where $R^t = ((-1)^{j(2)} l_2, \ldots, (-1)^{j(n-1)} l_{n-1})$. Then the Hessian G can be written $G = [C + (-1)^{j(1)} RR^t]$. Now G is a symmetric matrix, and, since all the diagonal minors of RR^t are 0 if they are at least 2×2, it is easily seen that the determinant of the diagonal minor in G which involves the first $k-1$ rows and the first $k-1$ columns is given as

$$(-1)^{j(1)+j(2)+\cdots+j(k)} l_1^{k-2} l_2 \cdots l_k \sum_{v=1}^{k} (-1)^{j(v)} l_v.$$

Explicitly, the sequence of diagonal minors of G is

$$\begin{matrix} (-1)^{j(1)+j(2)} l_2((-1)^{j(1)} l_1 + (-1)^{j(2)} l_2) \\ (-1)^{j(1)+j(2)+j(3)} l_1 l_2 l_3((-1)^{j(1)} l_1 + (-1)^{j(2)} l_2 + (-1)^{j(3)} l_3) \\ \vdots \end{matrix} \qquad 6.10$$

¿From this the result is immediate when we note that the signature of a symmetric non-singular matrix is given in terms of the sign of the first diagonal minor, and from then on the changes of sign in the diagonal minors above as k increases. ∎

§7: The structure of inverse images of curves

It turns out that we do not need the exact index of these critical points. What matters is how many of them there are in the inverse image of a given path in the workspace. But

before we get into these details we need to make a few remarks about the dependence of these inverse images on the particular path, γ.

Throughout this section we assume that the inequalities among the $l_1, \ldots, l_n$ required for the non-singularity of all the critical points are satisfied.

By assumption γ is differentiable with transverse intersections with the critical point circles (spheres) of the map from the (free) configuration space to the workspace. Assume that γ has been parameterized by (scaled) arc-length and is thus given by a (unique) differentiable map $I \longrightarrow W(l_1, \ldots, l_n)$. It follows that the union of these intersection points forms a discrete labeled configuration of points in I, where the labeling is by the radius of the particular critical sphere containing the image. Clearly, there is a single constraint on this set - adjacent labeled points must either be labeled by the same radius or by the next larger or smaller radius. But aside from this constraint any finite, discrete configuration of labeled points can arise. We call the resulting labeled configurations that actually arise *admissible configurations*. All the admissible configurations are naturally *ordered* via the natural ordering of the inverse images of the critical spheres in I, and thus, associated to each admissible configuration there is a unique ordered sequence of radii of critical spheres.

DEFINITION 7.1: *Two admissible configurations are equivalent if and only if the associated ordered sequences of radii of critical spheres are equal.*

The following result is now direct from 5.3.

THEOREM 7.2: *Let γ_1 and γ_2 be two admissible curves in the workspace $W(l_1, \ldots, l_n)$ with the same end-points which are not on the critical spheres. Then the inverse images of the two curves are diffeomorphic if their associated configurations of labeled critical points are equivalent.*

REMARK 7.3: It is clear that one does not actually need the endpoints of the two curves to be equal, merely that they lie in the interiors of the same annular regions between adjacent critical radii.

DEFINITION 7.4: *A curve γ is monotone if the associated ordered sequence of critical radii is monotone.*

In the case of monotone curves, in order to understand the diffeomorphism type of the associated inverse image, it is sufficient to assume that the curve is a segment of a ray from the origin, and we will concentrate on *monotone curves* - and consequently, segments on rays from the origin - in what follows.

EXAMPLE 7.5: Suppose that the base is a prismatic joint, which, for simplicity, we will assume simply means that the length of the base varies in the closed interval $[l_n(0), l_n(1)]$. Then the resulting configuration space will be the inverse image of the line segment $[l_n(0), l_n(1)]$ along the positive x-axis.

EXAMPLE 7.6: Suppose that we are interested in the inverse image of l_n along the x-axis, and suppose that l_n is not a critical radius. Then the configuration space $\mathcal{C}(l_1, \ldots, l_n)$ is non-singular and is the boundary of the inverse image of the segment $[l_m, l_1 + l_2 + \cdots + l_n]$.

Likewise, the union of the configuration spaces $\mathcal{C}(l_1, \ldots, l_n(0))$ and $\mathcal{C}(l_1, \ldots, l_n(1))$ is the boundary of the configuration space described in the first example for the prismatic joint.

EXAMPLE 7.7: When we bootstrap in the plane, and construct the configuration space

$$\mathcal{C}(l_1, \ldots, l_n)$$

by taking the inverse image of the intersection of the circle centered at l_n of radius l_1 with the free workspace for $(l_2, \ldots, l_{n-1})$ we break the intersection up into two pieces, the inverse image of the part of the circle above the x-axis and the inverse image of the part of the circle below it. Both of these are monotone and consequently diffeomorphic. We have just proved the following theorem:

THEOREM 7.8: *The configuration space of a closed chain in $\mathbb{R}^2$ is the double over the boundary of the inverse image of a monotone path and hence a segment along the x-axis.*

It remains to characterize these inverse images. In what follows we consider the inverse image of the line segment S along the x-axis from $l > 0$ to $\sum l_i$, the radius of the workspace, where l is not a critical value. We also assume that we are in $\mathbb{R}^2$ though the modifications in the argument below for $\mathbb{R}^3$ are direct.

Suppose that $r_I \in S$, then for each $j \in I$, the j-interval is parallel to the x axis and points inward. The itervals which are not in I of course point outwards, and leaving these intervals fixed while freely varying the intervals with $i \in I$ results in an annulus or a disc centered about the point $\sum_{i \notin I} l_i$ having exterior radius $\sum_{i \in I} l_i$ as the image of the endpoint.

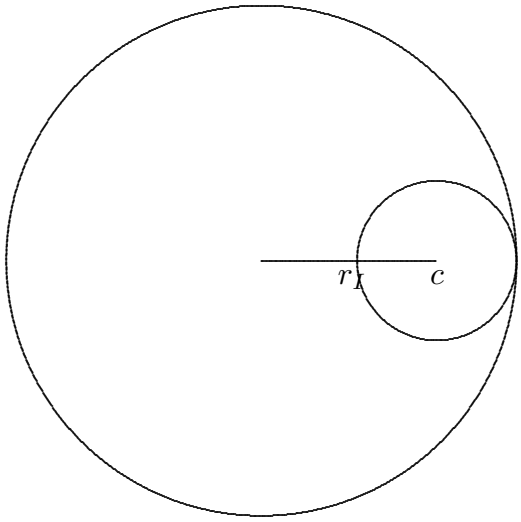

Figure 11: $c = \sum_{i \notin I} l_i$

Thus, to each critical value r_I in S there is associated a unique sub-coordinate torus, T^I, in the configuration space, and if $J \subset I$ then $T^J \subset T^I$. Moreover, for each coordinate subtorus of T^I there is a unique J so this subtorus is T^J, but these tori do not lie in $f^{-1}(S)$, instead the images of their endpoints lie in the small disk in Figure 11.

We now indicate how to construct a deformation retraction of the union of the sub-tori above to a sub-complex of $f^{-1}(S)$.

The angle subtended between the positive x axis and one of these endpoints always lies between $\frac{-\pi}{2}$ and $\frac{\pi}{2}$, and consequently defines a homotopy trivial mapping from this

sub-torus to the unit circle $S^1 \in \mathbb{C}$. It follows that we can construct a deformation retraction of the coordinate inclusion of this torus in the free configuration space to the inverse image of S by rotating each element by the negative of the angle the endpoint of the configuration makes with the x-axis. Thus, the entire torus $T^{|I|}$ consisting of points of the form $(\tau_1, \ldots, \tau_{n-1})$ with $\tau_i = 0$ for $i \notin I$ is represented by a torus in the inverse image of S.

Indeed, these deformation retractions agree on the intersections of the tori associated to different critical values and give, as claimed, a deformation retraction of the entire union to $f^{-1}(S)$.

REMARK 7.9: The deformation retraction, restricted to each torus separately is a diffeomorphism of that torus into S since we can find the angle that the original point made by looking at one of the edges which is not in I. Moreover, given any two I, J with r_I, r_J both in S, then $I \cup J$ is not $(1, 2, \ldots, n-1)$. Indeed, if it were then there would be two complementary subsets of the set of integers $\{1, \ldots, n-1\}$, I, and the complement of I, $C(I) = \{1, \ldots, n-1\} - I$ among the permissible J with $r_J \in S$. But $r_{C(I)} = -r_I$ and we assume that S is contained in the positive x-axis. Hence, there will be a $j \notin I \cup J$, so it follows that the deformation retraction actually is a homeomorphism on the union of these sub-tori.

If we take the union of these tori, we obtain a cell complex with exactly as many cells as there are critical points in the inverse image of S. Moreover, the image of the homology of the original union of sub-tori in the homology of the free configuration space $(S^1)^{n-1}$ is injective and has one independent generator for each critical value in S. Since the critical points are non-singular, we have accounted for every cell in the cell decompostion of $f^{-1}(S)$ associated to this Morse function. It follows that the deformation retraction of this union must be a deformation retract of the entire inverse image. This proves all of our main result except for the normal bundle data which describes the self-intersections under Poincaré duality.

§8: The completion of the proofs of 1.5and 1.8

We now consider the normal neighborhoods of these tori in $f^{-1}(S)$. Our assumptions remain the same as in the previous section.

LEMMA 8.1: *Let T^I be the torus associated to the critical point given by the subset $I \subset (1, \ldots, n-1)$ above, then, in $f^{-1}(S)$, the normal neighborhood of T^I is a product $T^I \times \mathbb{R}^j$ with $j = n - 2 - |I|$.*

PROOF: Let r_I be the critical value,

$$r_I = \sum_1^{n-1} l_i - 2 \sum_{j \in I} l_j$$

associated to I. Since l, the right hand boundary of the segment S, is not a critical value, there is an $\epsilon > 0$ the interval $(r_I - \epsilon, r_I]$ contains no other critical points and is contained in S.

We now look only at $f|_I$ by which we mean the mapping

$$f\colon (X_1, \ldots, X_{n-1}) \longrightarrow \sum l_i X_i$$

restricted to the edges l_v with $v \notin I$. The inverse image of the interval along the x-axis $(d-\epsilon, d)$ where $d = \sum_{j \notin I} l_j$ is an open disc $D^{n-|I|-2}$ since the only critical point is at d and this is clearly an absolute maximum. On the other hand, specifying any configuration in this disk, any configuration on the deformation of the torus into S, and adding together gives an element in $f^{-1}(S)$, since the angles are all equal for the edges which are not in I in the deformed torus. (This is the point where things change somewhat between $\mathbb{R}^2$ and $\mathbb{R}^3$, but the modifications are direct.) This proves the lemma. ∎

It remains to determine the structure of the union of two sufficiently small normal neighborhoods of two tori $T^I \times R^{j(I)}$ and $T^J \times R^{j(J)}$ in $f^{-1}(S)$. We have:

LEMMA 8.2: *Let $r_{max} = \sum_1^k l_s$, for a sequence of positive numbers $l_1, \ldots, l_k$. (Here we are considering proper subsets of our full set $(l_1, \ldots, l_n)$ and reordering.) Let*

$$(\vec{X}_1, \ldots, \vec{X}_k) \in (S^1)^k$$

and set $f(\vec{X}_1, \ldots, \vec{X}_k) = \sum l_i \vec{X}_i$. (Forward kinematics restricted to the subset.) Let $S = (r_{max} - \epsilon, r_{max})$ on the x-axis, and $f^{-1}(S) = D^{k-1}$, the open disc of dimension $k-1$. Then local coordinates in D^{k-1} can be given by choosing any $i \in \{1, \ldots, k\}$ and letting X_i depend on the remaining X_j, $j \neq i$.

PROOF: Write $X_i = (cos(\theta_i), sin(\theta_i))$. Then up to third order we have that f is given by

$$\hat{f}(X_1, \ldots, X_k) \;=\; \left(r_{max} - \sum_1^k l_i \theta_i^2, \sum l_i \theta_i \right).$$

Since all the $l_i > 0$ and the condition for being in S is $\sum l_i \theta_i = 0$ up to third order, the result follows. ∎

¿From this lemma and the preceeding result, the fact that a regular neighborhood of the union of any two tori is given in the way described in the introduction now follows. For $\mathbb{R}^3$ the argument and conclusion are the same.

§9. Closed chains with constrained points

In a sequel we will consider the structure of subspaces of these configuration spaces where we require either that there are no self-intersections in the chain or that the chain does not intersect a forbidden region. In order to do this we need a structure result for closed chains with a number of constrained interior points. As the key result involves exactly the same analytic techniques as were developed in §6, we include the conditions for non-singularity of such subspaces here.

We consider the situation where we also bind r distinct interior points on the chain, requiring them to be fixed.

LEMMA 9.1: *The configuration space of all configurations of a closed chain $\langle l_1, \ldots, l_n \rangle$ with l_n mapping to a fixed segment based at the origin and r points of the chain*

$$\{\vec{V}_1, \ldots, \vec{V}_r\} \subset \langle l_1, \ldots, l_n \rangle$$

required to satisfy $f(\vec{V}_i) = \vec{L}_i$, $1 \le i \le r$, is non-singular if and only if it is not possible to make all the edges between any two of the constrained positions collinear.

PROOF: The resulting set of equations has the form:

$$
\begin{aligned}
\sum_{1}^{n-1} l_i \vec{X}_i &= \vec{L}_n \\
\sum_{1}^{j_1-1} l_i \vec{X}_i + k_1 \vec{X}_{j_1} &= \vec{L}_1 \\
\vdots \quad & \quad \vdots \quad \vdots \\
\sum_{1}^{j_r-1} l_i \vec{X}_i + k_r \vec{X}_{j_r} &= \vec{L}_r
\end{aligned}
\tag{9.2}
$$

with $j_1 > j_2 > \cdots > j_r$. (Note that if $0 < k_i < l_i$ then the binding point for the i^{th} edge is *on* the edge, while if $k_i = 0$ or $k_i = l_i$ the binding point is a vertex. However, it is also possible for k_i to be negative or $k_i > l_i$ in these equations, and, though these last are not part of the statement of 9.1, the discussion below does not change in these cases. The Jacobian here has the form

$$
\begin{pmatrix}
2x_1 & \dots & 0 & \dots & 0 & 2y_1 & \dots & 0 & 2z_1 & \dots & 0 \\
\vdots & \ddots & \vdots & \ddots & \vdots & \vdots & \ddots & \vdots & \vdots & \ddots & \vdots \\
0 & \dots & 0 & \dots & 2x_{n-1} & 0 & \dots & 2y_{n-1} & 0 & \dots & 2z_{n-1} \\
l_1 & \dots & l_{j_1} & \dots & r_{n-1} & 0 & \dots & 0 & 0 & \dots & 0 \\
0 & \dots & 0 & \dots & 0 & l_1 & \dots & l_{n-1} & 0 & \dots & 0 \\
0 & \dots & 0 & \dots & 0 & 0 & \dots & 0 & l_1 & \dots & l_{n-1} \\
l_1 & \dots & k_1 & \dots & 0 & 0 & \dots & 0 & 0 & \dots & 0 \\
0 & \dots & 0 & \dots & 0 & l_1 & \dots & 0 & 0 & \dots & 0 \\
0 & \dots & 0 & \dots & 0 & 0 & \dots & 0 & l_1 & \dots & 0 \\
\vdots & \ddots & \vdots & \ddots & \vdots & \vdots & \ddots & \vdots & & \ddots & \vdots
\end{pmatrix}
\tag{9.3}
$$

and the reduction above results in triples of the form

9.4
$$\begin{pmatrix} 2x_i & 0 & 0 \\ 0 & 0 & 0 \\ \vdots & \vdots & \vdots \\ 0 & 0 & 0 \\ l_i & a_{i,1} & b_{i,1} \\ 0 & a_{i,2} & b_{i,2} \\ 0 & a_{i,3} & b_{i,3} \\ l_i & a_{i,1} & b_{i,1} \\ 0 & a_{i,2} & b_{i,2} \\ 0 & a_{i,3} & b_{i,3} \\ \vdots & \vdots & \vdots \\ 0 & 0 & 0 \\ \vdots & \vdots & \vdots \\ 0 & 0 & 0 \end{pmatrix}$$

where the number of non-zero vertical copies of the two vectors is the number of times that $\vec{X}_i$ occurs with non-zero coefficient in the equations above. Consequently, the resulting variety is non-singular if and only if it is impossible to make all the edges between any two of the constrained positions colinear, as asserted. ∎

Bibliography

[C] J. F. Canny, *The Complexity of Robot Motion Planning*, Thesis, MIT, 1987.

[H] K.H. Hunt, *Kinematic Geometry of Mechanisms*, Oxford University Press, 1978.

[KM1] M. Kapovich, J. Millson, On the moduli spaces of polygons in the Euclidean plane, *Journal of Diff. Geometry*, **42** (1995), 133-164.

[KM2] M. Kapovich, J. Millson, The symplectic geometry of polygons in Euclidean space, *Journal of Diff. Geometry*, **44** (1996), 479-513.

[KM3] M. Kapovich, J. Millson, Universality theorem for configuration spaces of planar linkages, *Preprint, U. of Utah*, (1998).

[KLOS] L.E. Kavraki and P. Švestka and J.-C. Latombe and M.H. Overmars, Probabilistic Roadmaps for Path Planning in High-Dimensional Configuration Spaces", *IEEE Transactions on Robotics and Automation*, **12**, (1996), 566–580.

[SM] G. Shukla and A.K. Mallik, Detection of a crank in six-link planar mechanisms, *Mechanism and Machine Theory*, **35**, (2000), 911–926.

[WXH] P. Watterberg, P.Xavier and Y. Hwang, Path Planning for Everyday Robotics, *icra*, (1997), 1170–1175.